

# “Earthquake Protection of Colonial Bell-Towers in Colima, Mexico with Externally Prestressed FRPs”

Adolfo Preciado<sup>1</sup>, Harald Budelmann<sup>2</sup> and Gianni Bartoli<sup>3</sup>

<sup>a</sup> Departamento del Hábitat y Desarrollo Urbano, Instituto Tecnológico y de Estudios Superiores de Occidente (ITESO), Tlaquepaque, Jalisco, México

<sup>b</sup> Institut für Baustoffe, Massivbau und Brandschutz, Technische Universität Braunschweig (TUBS), Braunschweig, Germany

<sup>c</sup> Dipartimento di Ingegneria Civile e Ambientale, Università degli Studi di Firenze (UniFI), Firenze, Italy

## ABSTRACT

A methodology for the seismic vulnerability reduction of old masonry towers with external prestressing is presented. It is applied at the Colonial bell-towers of the Cathedral of Colima, Mexico, characterized for being a high seismic area ( $M > 7.5$ ). The 3D FE models are calibrated with experimental data and assessed through nonlinear static approaches including the seismic demand and an accurate validated masonry model. Based on an extensive parametric study on different configurations of old masonry towers, it is selected an optimal prestressing force and device. The Colonial towers are retrofitted with four prestressing devices of FRPs to convert them into a high energy-dissipative reinforced masonry. The external vertical prestressing is included at key points identified in the seismic vulnerability assessment. This technique is in compliance with the demand for architectural conservation and may be located without drilling and unbounded in order to be fully removable. The seismic performance is enhanced by increasing force, displacement and internal confinement. It is observed an upgrading of 35% and 20% of displacement capacity. With these results it is corroborated that external vertical prestressing allows a substantial increment of ductility for seismic energy dissipation purposes.

**Keywords:** *Strong earthquakes; bell-towers; historical masonry; nonlinear assessments; retrofitting; unbounded prestressing; FRP devices; energy dissipation*

## **1. INTRODUCTION**

Earthquake (EQ) protection of ancient buildings is an issue of intensive research in recent years. The main difficulties on the seismic analysis and strengthening of these buildings arise from the high heterogeneity and heavy weight of masonry and great thicknesses to support the vertical loading induced by the massive structure. Moreover, the low tensile strength of masonry induces cracking mainly by shear and flexion since very low lateral loads and tends to separate the structure into macro-blocks that behave independently with different failure modes. Degradation of masonry through time (long-term heavy loads) is another important factor affecting the seismic behavior of old buildings. These tall and massive structures may present a complete failure even in static conditions when the concentrations of stresses overpass the intrinsic compressive strength of the material. This effect was the trigger on the collapses of the bell tower of “Piazza San Marco”, Venice (1902), the civic tower of Pavia (1989) and the bell tower of the church of “St. Maria Magdalena” in Goch, Germany (1992). All these factors in combination with the EQ source, frequencies and local site effects, make the seismic analysis and the remedial measures to attain the protection of this type of structures a complex task.

Nowadays there is an enormous variety of methods to assess the seismic risk of buildings (Carreño et al. 2012). The main objective is to assess the seismic risk of a certain building or group of buildings in a satisfactory way and to study the corrective measures for reducing that risk. The seismic risk of a historical structure located in a seismic zone is determined by the conjunct of the seismic hazard and its structural vulnerability. Recent studies in EQ engineering are oriented to the development, validation and application of techniques to assess the seismic vulnerability of existing buildings (Carreño, et al., 2007; Barbat, et al., 2008; Lantada, et al., 2009 and Pujades, 2012).

## **2. EARTHQUAKE PROTECTION OF HISTORICAL MASONRY STRUCTURES**

Nowadays, there is a huge variety of techniques and materials available for the protection of historical masonry constructions. Among them, two main techniques are distinguished, the rehabilitation (restoration) and the retrofitting (upgrading). The rehabilitation aims to use materials of similar characteristics to the originals to locally correct the damage of certain structural elements to preserve the building in good conditions and its vertical load carrying capacity. By the other hand, retrofitting intends to use engineering techniques and advanced materials to mainly improve the seismic performance of the building by increasing its ultimate lateral load capacity (strength), ductility and energy dissipation. Compatibility, durability and reversibility are the fundamental aspects recommended in literature to be taken into account when retrofitting is applied for the seismic protection of cultural heritage. Moreover, a good compatibility of deformations between materials is important in order to avoid a stress concentration that could generate damage to the rest of the structure.

Since the seismic hazard is unavoidable and it is not in our hands to reduce it or modify it, therefore this research work is aimed at reducing the structural vulnerability of historical towers by the implementation of external prestressing devices in order to attain the seismic risk reduction. Assessing the seismic vulnerability of a historical building is a complex task if compared to other existing or new building as explained in the works of Barbieri et al. (2013), Foraboschi (2013), Preciado et al. (2014) and Preciado and Orduña (2014). The recommended procedure consists of obtaining at a first instance all the relevant information such as identification of structural elements, damages, plans, historical analysis and restorations, as well as experimental vibration tests. Furthermore, with the obtained information is possible to construct a 3D geometrical model with computational tools. After building the initial 3D model (e.g. finite element, limit analysis, etc.), the mechanical properties of materials constituting the

structure and boundary conditions are assigned. Together with a suitable constitutive material model able to satisfactorily represent the nonlinear behavior of unreinforced masonry (URM), the model is statically or dynamically assessed. These evaluations are linear or nonlinear depending on the aim of the study and the action under analysis (e.g. self weight, seismic loading, wind, etc.) in order to define the levels of damage in the structure (vulnerability).

Once the seismic vulnerability of the building has been assessed satisfactorily, the technique of prestressing may serve as retrofitting in order to improve the overall seismic capacity of the historical construction. In this research, the devices are vertically and externally located at key locations inside the towers in order to give to the retrofitting the characteristic of reversibility, respecting in all senses the architectonic and historical value of the structure. The post-tensioned devices intend to improve the seismic performance of the towers by reducing damage with the application of a pre-compression to the masonry at key locations of the structure. The pre-compression allows reducing the tensile stresses and obtaining with this a better confinement, ductility and strength enhancement against lateral loading. This enhancement allows more seismic energy dissipation, achieving the seismic risk reduction.

Both bell-towers of the Cathedral of Colima "*Basílica Menor de Guadalupe*" (Figs. 1 and 3) are selected as case study of this research because of the strong observed damage due to historical EQs, showing once almost a total collapse of the left tower (Fig. 1a). The Cathedral is located in the historical center of Colima City (Fig. 2) and approximately built in 1889 with two bell-towers at the main façade. The building is considered as the most important Colonial monument of Colima by its great historical and cultural value.

### **3. SEISMIC HAZARD CHARACTERIZATION OF COLIMA, MEXICO**

The state of Colima is located in the Mexican Littoral in the Pacific Ocean with an extension of 5455 km<sup>2</sup> and adjoins with the states of Jalisco in the NW direction and with Michoacan in the SW. At national level, the seismic hazard of Mexico is divided in four main zones ranging from A to D, where A represents low hazard and D very high. In the seismological context Colima is distinguished by its important exposure (seismic zone D), being considered one of the Mexican states under most significant hazard (Fig. 2). Bandy et al. (1995) and Ramirez-Gaytan (2008) describe that the seismic hazard of Colima is determined by three main sources: the active Volcano of Colima that generates constant microseismicity ( $M < 3.5$ ); the Jalisco block located between the Rivera and North American plates and the convergence zone between the Cocos, Rivera and North American plates in front of the coastal area (see Fig. 2b). Mexico is located in the Circum-Pacific Ring, characterized by its high seismicity interplate. The seismic activity is generated by the convergence of the Cocos and North American plates (6 cm/year in average) and the Rivera and North American plates (4.5 cm/year) (Bandy et al., 1995). In the boundaries between plates have occurred major to great EQs causing strong damage to the cities of Manzanillo, Tecoman, Colima, Guadalajara and Mexico (see Table 1). Historically, Colima has been subjected to strong EQs of more than M7.5 and intensities ranging from VII to X. The most recent strong events that have affected the region occurred on October 9<sup>th</sup>, 1995 with M8 and on January 21<sup>st</sup>, 2003 M7.5 (Table 1). According to the Mexican codes MDS-CFE (2008) and NTCDF (2004), as well as the seismic hazard characterization developed at the historical center of Colima City, it is classified as soil type I (stable) and high seismic hazard zone D, with a maximum PGA value (rock site) of 0.50g ( $a_0$ ) with a probability of exceedance of 10% in 50 years and a return period of 475 years. Table 2 presents the summary of the needed parameters to develop the normalized elastic response spectrum.

#### **4. HISTORICAL ANALYSIS AND CONSERVATION STATE OF THE TOWERS**

The Cathedral of Colima was approximately built in 1889, two years later it was finished the construction of the adjacent chapel. The materials used for its construction were fired clay bricks and carved stone with lime mortar for all the vertical elements such as walls and towers and empty fired clay basins in a matrix of mortar for the vaults. Colima City has been subjected to strong EQs due to its proximity to an important seismic source as described in the seismic hazard characterization. About 10 years after its construction the building was damaged by an EQ, presenting moderate damage at both towers and cupola but strong non-structural damage. In 1941 occurred a M7.6 EQ generated by the subduction of the Cocos plate beneath the North American plate. The strong ground motion was felt in the city with an intensity of X (Table 1). It highly damaged the building, generating important cracking at walls, cupola, vaults and the partial collapse of the left tower. The belfry collapsed almost totally, falling down in a highly transited street (see Fig. 1a), causing for luck just small injuries to some pedestrians. For the tower's reconstruction, materials with similar characteristics were used. Afterwards, in 2003 the city was struck again by another important EQ with the same rupture mechanism of the occurred in 1941. The M7.5 EQ was felt this time with lower intensity (VIII) but caused strong damage to the entire building especially at both bell-towers (see Fig. 1b). The restoration and strengthening works were developed by INAH (2003). The wall thickness was increased by adding thin concrete walls. The vaults were strengthened with a steel mesh covered by mortar and some reinforced concrete beams were included at the level of belfries. Nowadays, the complete Cathedral is in a good conservation state as illustrated in Figure 3a thanks to the 2003 interventions which have shown good performance after recent moderate seismic events.

## 5. STRUCTURAL CHARACTERIZATION BY EXPERIMENTAL CAMPAIGNS

The main structural components of the Cathedral were described in Section 4. There is no information available regarding the structural characteristics in terms of mechanical and dynamic data. During the intervention works developed by INAH (2003), the experimental campaigns were limited to characterize the type of materials of the different structural components by non-destructive sampling. The strengths of materials were not assessed, nor the level of stresses at vertical elements and dynamic characteristics. During the present research work several technical visits were developed in order to assess by visual inspections the actual conservation state of the building. Moreover, the dynamic characteristics of the bell towers under study (left in Fig. 3a) are assessed. The natural frequencies were obtained by means of a portable vibration analyzer (triaxial accelerometer) CSI RBM Consultant<sup>®</sup>, consisting in one sensor and its data acquisition control (Fig. 3b). The used excitation was induced by means of ambient vibration (traffic and wind) and registered at the bell-tower at a height of 31 m at the upper level of belfry (Fig. 3). Afterwards, from the acquisition control, the registered data was transferred to a computer and managed with especial software. By means of the vibration spectra, the natural frequency is graphically determined. The results of the two orthogonal directions are 1.4067 Hz in the E-W (transversal) direction and 1.6222 Hz in the N-S (longitudinal). The Spanish Standard NCSE (2002) proposes an analytical formula to approximately assess the first frequency  $\omega$  of masonry bell towers (see Eq. 1). Where  $L$  corresponds to the plan dimension in the vibration direction and  $H$  is the height of the towers. The suitability and efficiency of this equation as a first and quick estimation (or validation of numerical and experimental results) of the first natural frequency of real masonry bell towers have been proved by many researchers, e.g. Ivorra and Pallares (2006), Ivorra et al. (2008) and Bayraktar et al. (2009).

$$\omega_1 = \frac{\sqrt{L}}{0.06 H \sqrt{\frac{H}{2L + H}}} \quad (\text{Hz}) \quad (1)$$

By means of the use of Eq. 1 (L= 6 m, H= 31 m), a first natural frequency of each tower of 1.5508 Hz or higher is expected due to the interaction with the Cathedral. In order to obtain models more representative of the real structure and more reliable results in the seismic risk management, they are calibrated with experimental data and the process is described in the following section.

## 6. CONSTRUCTION OF FE MODELS AND CALIBRATION

The seismic analyses by finite element (FE) models of the bell-towers of the Cathedral of Colima are developed considering two directions (-X and +X) and the respective calibrated models with experimental data. Due to symmetry, the left tower was selected for the analyses and no considerable changes are expected in the other two directions (-Y and +Y). In the +X model (see Fig. 7) the interaction with the façade (South, L= 4 m and 105 springs) and the nave (East, L= 2 m and 63 springs) up to the height of 20 m is considered by a horizontal distribution of linear elastic springs (Combin14) with constant stiffness. To simulate the interaction induced by neighbor masonry buildings it is proposed Ec. 2, based on the works of Pandey and Meguro (2004), Crisafulli and Carr (2007) and Mondal and Jain (2008), where the authors assess the lateral stiffness contribution on masonry infill panels. The axial spring stiffness  $K_{sp}$ , is assumed to be equal to a fraction  $\gamma$  of the total stiffness of a masonry block.

$$K_{sp} = \gamma \frac{E_m A_m}{T_m} \quad (2)$$

Where  $E_m$  is the elastic modulus of masonry,  $A_m$  is the area of a composite masonry block of 1x1 m (4 springs) and  $T_m$  is the wall thickness. The factor  $\gamma$  is recommended by other researcher to be



estimated between 0.50 and 0.75 depending on the author when calibrating the model. During the calibration process it is decided to use a factor of 0.30, resulting in a spring stiffness of 100 kN/mm. This value is in good agreement with the proposed by Ivorra and Pallares (2006), where the authors experimentally evaluated the lateral stiffness contribution of masonry façades in old bell-towers. The -X model (see Fig. 5) is proposed without springs in order to simulate a disconnection with the façade and nave. The tower has a square plan of 6 x 6 m with a wall thickness of 1.5 m and 31 m height. With the cover (0.10 m thick) the tower has a total height of 37 m and a reinforced concrete slab at belfry (total mass of the structure of 1707.4 Ton). The 3D FE models are integrated by 859 Shell43 elements and 906 nodes with 5367 degrees of freedom (DOF) and developed by the commercial software ANSYS®. The mechanical properties for both models are defined taking into account similar historical constructions and typical values reported in literature for defining the elastic behavior. By means of the reports of INAH (2003) it was observed that the façade is formed by brick masonry with lime mortar and both towers with brick and carved stone masonry at different heights. In the analysis is considered a density of 1.6 ton/m<sup>3</sup> (brick masonry) and 2 ton/m<sup>3</sup> (carved stone), a compressive strength of 2.5 MPa, tensile strength of 0.25 MPa Young's modulus of 2000 MPa. The Poisson's ratio is held constant and equal to 0.15.

### **6.1 Calibration of the numerical FE models with real experimental data**

In the generation of the initial FE models there are several assumptions and uncertainties regarding the determination of geometry, material properties, support and boundary conditions. Due to this, the initial analytical models may be compared with real physical characteristics of the structure. The models are calibrated or updated through modal analyses by modifying masonry elastic modulus, density and spring stiffness. After following an iterative approach, the

numerical and experimental frequencies are in good agreement as presented in Table 3. Moreover, the towers are subjected to vertical loading analysis to verify the model by comparing the sum of forces at the supports with the total vertical force, as well as to verify the distribution of stresses (compression and tension). Both towers are as expected subjected to compressive stresses concentrated at the base, but in any case higher than the intrinsic strength.

## **7. NONLINEAR STATIC EARTHQUAKE ANALYSES OF THE TOWERS**

Nonlinear static analyses (pushover) relate the resistance and energy-dissipation capacity to be assigned to the structure to the extent to which its non-linear response is to be exploited. Therefore, non-linear static analyses account for both the actual force-resisting system of the building, in particular the overstrength, and the actual energy-dissipation system of the building, in particular not only the plastic dissipation (Foraboschi and Vanin, 2013a). In the case of masonry buildings, moreover, linear analyses suffer from the absence of correlation between linear behavior and ultimate limit state. More specifically, the stress results of a linear analysis are not significant, since a masonry structure does not fail due to excessive stresses but due to a mechanism (either rotating or translating) (Blasi and Foraboschi, 1994).

The FE models are subjected to linear analyses in Section 6. These preliminary evaluations serve to verify the load carrying capacity of the towers and distribution of stresses, as well as to compare the numerical frequency with the experimental one for model calibration/updating.

The EQ assessments of both masonry towers of the Cathedral of Colima are developed through the Pushover technique following a displacement load pattern assuming that the towers behave as cantilever beams of 1 DOF. The horizontal force is applied under monotonically increased top displacement control at the bell-tower at a height of 31 m at the upper level of belfry (Fig. 3a).

The expected main failure mechanisms of historical masonry towers under static lateral loading

are integrated by (1) bed joint sliding, (2) stepped cracking by low vertical loading (through head and bed joints), (3) diagonal cracking by high vertical loading (through joints and units), (4) horizontal cracking and rocking by bending and (5) masonry crushing.

The selection of a suitable material model depends on the seismic analysis method, importance of the building, available data and reliability of the expected results. In the framework of the FE analysis, three main modeling strategies for masonry are identified to be the most used in the relevant literature. The micro-modeling (discrete) of single elements (unit, mortar and interface) and meso-modeling (unit and interface), are suitable for the analysis of small structures, e.g. Lofti and Shing (1994) and Lourenço and Rots (1997). The large amount of time for the generation of the detailed structural model and high calculation effort prevent their use in the seismic analysis of sophisticated and large-scale structures as in the case of historical constructions. By the other hand, the macro-modeling (smeared, continuum or homogenized), considers masonry as an anisotropic composite material, e.g. Gambarotta and Lagomarsino (1997), Lourenço et al. (1998) and Schlegel (2004). This simplifies the generation of the structural model, and due to the significantly reduction of the degrees of freedom, less calculation effort is needed, being considered as a suitable for the seismic analysis of large historical constructions.

Macro-modeling of masonry through analytical models is also gaining the attention of the scientific community for static nonlinear analysis purposes. Among them are the 3D limit analysis approach by rigid macro-blocks (Orduña and Lourenço, 2005a and b) (Orduña et al. 2008) and the strut-and-tie model (Foraboschi and Vanin, 2013a). The first approach is based on a rigid-perfectly plastic material that does not need parameters of stiffness and softening, only strength parameters. By the other hand, is not possible to evaluate the displacements and deformations of the structure, which are fundamental for seismic energy dissipation assessments.

The strut-and-tie modeling approach was developed for reinforced concrete members and can include externally reinforced concrete members (Biolzi et al., 2013). The strut-and-tie modeling approach is supported by the lower bound theorem of the limit analysis, as well as by the maximum stiffness or minimum deformation energy criteria (Blasi and Foraboschi, 1994). Actually, the original form of the lower bound theorem refers to an elasto–plastic constitutive law of the material, which does not include masonry. However, the lower bound theorem can be extended to masonry structures, under the assumption that masonry has an elasto-plastic compression behavior (or perfectly elastic) and a no-tension behavior, which is an assumption that suits masonry adequately (Foraboschi and Vanin, 2013a).

However, FE modeling is still the most powerful tool and recommended to assess the vulnerability of large historical constructions against EQs. This is due to its capability to calibrate the model by means of modal analysis and the obtained real frequencies obtained by ambient vibration tests at the structure. Moreover, analytical models are not capable to simulate nonlinear dynamic analysis, disregarding the EQ characteristics, damping and dissipation of energy by interlocking and opening-closure of cracks.

### **7.1 Nonlinear static analyses by the Pushover method**

In the nonlinear analyses through FE models, the homogenized masonry material model developed by Gambarotta and Lagomarsino (1997) is implemented. This material model is capable to simulate the main failure mechanisms and behavior of masonry structures in static and dynamic conditions. This accurate material model has been validated by theoretical background and reported experimental examples in the research work of Preciado (2011). The constitutive model is integrated in the commercial finite element program ANSYS® by subroutines and based on the macro-modeling approach which is considered as appropriate for the seismic assessment

of large historical constructions. Furthermore, the suitability of the material model in masonry structures has been proved through numerical simulations against experimental results e.g. Calderini and Lagomarsino (2006). The continuum damage model is based on a micromechanical approach where masonry is assumed as a composite medium made up of an assembly of units connected by bed mortar joints. The contribution of head joints is not considered. The constitutive equations are obtained by homogenizing the composite medium and on the hypothesis of plane stress condition. The failure limit states for mortar and unit damage are depicted in Figure 4. The homogenised model is characterized by three yield surfaces determined by tensile failure and sliding of mortar joints considering the Coulomb friction law and compressive failure of units. In summary, if tensile stresses act in mortar bed joints  $\sigma_y \geq 0$ , three damage mechanisms may become active: failure of units, sliding and failure of mortar bed joints. By the other hand, if mortar joints are under compressive stresses  $\sigma_y < 0$ , then both damage mechanisms of units and mortar are activated.

The needed masonry material parameters are described in Table 4. In order to assess the seismic response of an historical building is recommended to obtain the material parameters through detailed experimental campaigns. This is always a complex task, mainly due to the heterogeneity of masonry, the lack of representative samples and the need of non-destructive tests. In case that it is not possible to obtain all the material parameters, the ones proposed and calibrated through numerical simulations by Preciado (2011) are recommended. However, these material parameters may be carefully selected because the response of the numerical model is very sensitive to them.

After the successfully application of the horizontal force under monotonically increased top displacement control at the bell-tower, it is possible to obtain the complete capacity curve and failure mechanisms during the analysis, especially to capture the nonlinear (plastic) range. The

failure mode at ultimate limit state (ULS) of the tower without springs for a seismic action in the  $-X$  direction is presented in Figure 5a. It is worth noting several flexural cracks at the lower part of the body and failure of belfry by a combination of flexural cracks out-of-plane and shear in-plane. The model with springs ( $+X$  direction) is stiffer as expected due to the interaction with the façade, presenting the failure of belfry by shear cracks (Fig. 6a). This brittle behavior is due to the large openings and the short column effect which reduces the flexural height of slender structures. The obtained failure mechanisms through numerical simulations are in complete agreement with the observed after real EQs and are characteristic of bell-towers (flexural cracks at body and shear at belfry). The different seismic performances of both models could be observed at the capacity curves illustrated in Figure 7. It is worth noting that the left tower under seismic action in  $-X$  direction presents at ULS a maximum displacement of 100 mm and a lateral force of 2741 kN. Compared to the brittle constrained  $+X$  model, the  $-X$  model presents its characteristic bending behavior due to the disconnection with the façade, represented by 25% of more displacement capability (see Table 5). The  $+X$  model is more resistant to horizontal loading (12%), but less ductile, which is not relevant for seismic energy dissipation purposes, it is more important to reach more ductility with no brittle failure. For this purpose, the technique of prestressing is quite helpful to reach a seismic upgrading of URM structures by increasing strength, ductility and internal confinement.

In order to have comparative indicators of performance it is included at the capacity curves the EQ performance limit states established by the European Code (EC-8) (Eurocode 8, 2004); the damage limit state (DLS) at first yielding; significant damage limit state (SDLS) representing significant damage and the ultimate limit state (ULS) near collapse. Moreover, these limit states at the capacity curves are correlated to the damage grades (DG) DG2, DG3 and DG4 proposed by

the European Macroseismic Scale (EMS-98) reported in Grünthal (1998). For having quantitative indicators of performance at the capacity curves, it is included the seismic coefficient (CS) determined by the ratio between the ultimate lateral force and the vertical loading. The seismic coefficient is typically expressed as a fraction or percentage of the gravity ( $g$ ). The main drawback of this indicator is that only the lateral strength of the structure is evaluated, disregarding the displacement and ductility which is extremely important in the EQ assessment of structures for energy dissipation capabilities (see Tables 5 and 6).

## **7.2 Nonlinear static analyses by the Capacity Spectrum method**

For assessing the seismic performance of the historical masonry bell-towers, the Capacity Spectrum (CS) method proposed by Fajfar (2000) is used. The aim is to graphically identify the performance point by the intersection between the capacity curve transformed into an equivalent SDOF system and the seismic demand represented by the elastic spectrum properly reduced. Figure 9 illustrates the converted capacity curves of the  $-X$  (disconnected) and  $+X$  (constrained) models, as well as the elastic response spectrum based on the seismic hazard characterization of Section 3. Since  $T^* > T_c$ , the target displacement is directly obtained without reducing the elastic response spectrum. Figure 9 illustrates the transformed capacity curves into bilinear curves of the  $-X$  and  $+X$  model for computing the ductility available against the seismic demand. The maximum reached displacement  $d_m^*$  for both models ( $-X$  and  $+X$ ) is not enough to withstand the seismic demand represented by the target displacement  $d_t^*$  (performance point). The maximum performance of the  $-X$  model is of about 19% less than the required performance and even more drastic the  $+X$  model with a poor performance in the order of 40% (Table 7). The  $-X$  model fails more ductile than the  $+X$  model as depicted on Figures 5a and 6a. The  $+X$  model presents flexural cracks at the lower part of the body and failure of belfry by a combination of bending

and shear stresses that allowed it to perform better than the +X model, which fails by shear stresses at belfry.

## **8. EARTHQUAKE PERFORMANCE UPGRADING BY EXTERNAL PRESTRESSING**

The technique of prestressing has been successfully used to improve the seismic behavior of concrete structures since the beginning of the XX century. The adaptation of this technique to the seismic retrofitting of cultural heritage has gained in recent decades especial interest for many researchers around the world. Post-tensioning (or prestressing) of masonry has shown to improve ductility and strength successfully as explained in the works of Ganz (1990) and (2002).

The technical solution that may be adopted to obtain a dissipative structure that adequately reduces the forces due to the elastic spectrum consists of transforming the masonry into high-dissipative reinforced masonry (Foraboschi, 2013). The most effective technique to convert (unreinforced) masonry into reinforced masonry is to epoxy bond Fiber-Reinforced Polymer (FRP) strips onto the external surface of the masonry (Ascione et al., 2005; D'Ambrisi et al., 2013a and b; Foraboschi and Vanin, 2013b; Muciaccia and Biolzi, 2012 and Fedele et al., 2014). Since historical buildings must be retrofitted with reversible techniques for not affecting its architectonic value (the bare-surface has to be kept unchanged), no plaster and FRP strips may be applied on the masonry. Therefore the need of another technique such as prestressed tendons is highly recommended in the relevant literature, Indirli (2001), Castellano (2001), Sperbeck (2009) and Preciado (2011). One solution that may be implemented is the external or internal prestressing by means of tendons and anchorage system at key points of the structure identified at the seismic vulnerability assessment. This technique is in compliance with the demand for architectural conservation and may be located horizontally and vertically without bonding in order to be fully removable. Moreover, external prestressing is more economic than internal



prestressing because it does not need masonry drilling, which damages the structure and needs specialized and expensive equipment. The no-bonding condition allows the further calibration and control of changes in prestressing forces by relaxation of the material and volumetric changes under climatic conditions.

### **8.1 Seismic retrofitting of historical masonry towers**

Even when external prestressing has been frequently used as seismic retrofitting measure of cultural heritage (Preciado, 2011), very few applications of this technique can be found in historical masonry towers. Past intervention techniques used in ancient masonry towers have been used more as local strengthening (to avoid out-of-plane failure) of certain vulnerable structural parts than for a real improvement of the global behavior of the structure against EQs. This is consequence of the limitations in the existing materials in those periods added to the lack of technology and knowledge about the real behavior of these structural elements. One of the few cases reported in literature is related to the strengthening of the General Post Office clock-tower in Sydney, Australia. The retrofitting intervention was finished in 1990 aimed at increasing its global seismic performance by means of vertical and horizontal prestressing with steel tendons in drilled holes with prestressing forces of 1771 kN (Ganz, 2002). Another famous real application of prestressing in bell-towers corresponds to the tower of the church of San Giorgio in Trignano, Italy. The bell-tower was strongly damaged by the 1996 M4.8 EQ. A combination of devices such as steel tendons and shape memory alloys (SMA) were vertically installed and without drilling at the four internal corners of the tower aimed to increase its bending and shear resistance. The combined devices were anchored at the top and foundation of the tower and post-tensioned with a prestressing force of 20 kN (80 kN total force). The retrofitting was verified by the occurrence of a similar EQ in 2000 with no damage of any type as explained in the works of

Indirli et al. (2001) and Castellano (2001). However, in both real applications the retrofitting was validated in qualitative terms with no numerical simulations. Moreover, the way of determining the post-tensioning force is not mentioned and the use of a combination of a high resistance material such as prestressing steel with an extremely poor material such as masonry is doubtful in terms of compatibility of deformations and stresses concentration.

In the context of this paper, a prestressing device is a structural member axially stressed in tension and is integrated by three main parts, the top and bottom anchorages and the tendon. The prestressing devices are vertically and externally located at key locations inside the towers in order to give to the retrofitting the characteristic of reversibility (removable), respecting in all senses the architectonic and historical value of the structure. Compatibility, durability and reversibility are fundamental aspects recommended in literature to be taken into account for the seismic retrofitting of cultural heritage. Reversibility is definitely the most important aspect, because if the applied technique shows deficiencies in terms of compatibility and durability that increase the seismic vulnerability of the structure or there is a new material/technique that allows a better seismic performance, this old retrofitting could be substituted by the new one. In order to conform to the fundamental requirements of structures under seismic action, the EC-8 specifies that at ULS shall be checked the ultimate capacity of the retrofitting device in terms of strength and deformability, in order to avoid an exceedance. Horizontal external prestressing has been mainly used in the cultural heritage to provide stability out-of-plane of walls or to reduce the tensile stresses generated by supports opening of vaults, arches and domes. By the other hand, vertical external prestressing has proved to be more suitable to increase the in-plane lateral strength and ductility of masonry walls by providing tensile strength at key locations. The level of improvement strongly depends on the level of the prestressing force, so, the higher the

prestressing force the higher the lateral strength and ductility. Especial careful may be taken into account in order to use this technique in historical masonry towers. Firstly, an optimal prestressing level may be designed, due to high prestressing levels could lead to local damage at the top anchorage zone, or a sudden collapse even in static conditions by an exceedance of compressive stresses at the bottom. Moreover, in seismic conditions, the compressed in-plane and out-of-plane toes (base) could fail by crushing and leading to a brittle failure.

## **8.2 Seismic upgrading of the Colonial historical masonry towers**

From an extensive parametric study on different configurations of old masonry towers Preciado (2011) proposes an optimal prestressing force and device that may be used in any compact or slender masonry structure ranging from light houses, medieval, civic and bell-towers with large openings at belfries (bells place). The parametric study included different tendon material such as conventional prestressing stainless steel, FRPs (Aramid and Carbon) and different SMAs. The last is also called NiTiNol (Nickel-Titanium) and presents a super elastic (or pseudo elasticity) behavior. This material can undergo very large deformations in loading and unloading cycles without permanent deformations forming a loop representing dissipation of energy. This superelastic material has found very interesting applications as seismic retrofitting of cultural heritage. The main goal of the parametric study was the investigation of the impact on the seismic performance of different parameters such as tendon material (steel and FRPs) and combinations with segments of SMAs, prestressing level, changes in tendon forces and SMA superelasticity.

Taking into account the parametric study, the Colonial towers of this research are retrofitted with four prestressing devices (anchorage plate and tendon) of FRPs. Compared to prestressing steel, FRPs are more resistant to corrosion, equal or superior tensile strength, insensitivity to electromagnetic fields, 15 to 20% lighter and the possibility to incorporate optical fiber sensors

for monitoring purposes. The disadvantages of FRPs are their vulnerability to fire and brittle failure with no yielding, showing a stress-strain behavior linear at all stress levels up to the point of failure. The recommended prestressing force is of about 40% of the ultimate load capacity for Aramid (AFRP) and 60% for Carbon (CFRP) due to the stress-rupture limitations. It is proposed four tendons of Technora AFRP because its low elasticity modulus is compatible with the poor one of historical masonry and has shown a very good enhancement in strength and ductility in the parametric study. The devices and anchorage system are made of the same AFRP material and vertically located in the interior part of the tower and anchored at the bottom and at the top (see Figure 3a). In order to apply in a uniform way the prestressing forces at the top anchorages and to avoid force eccentricities, it was applied a horizontal removable steel frame at the upper walls level (31 m). The total prestressing force is calculated taking into account percentages of the vertical loading of the tower. In this case the towers are retrofitted with four Technora devices and two prestressing levels because of the high seismicity of the region, 15% of vertical loading  $0.15F_v$  ( $A_t = 1000 \text{ mm}^2$ , 15 bars of 8 mm per tendon) and 30% of vertical loading  $0.30F_v$  ( $A_t = 2000 \text{ mm}^2$ , 30 bars of 8 mm per tendon).

The prestressing devices based on tendons are externally applied in the internal four walls of the towers without drilling and fully removable as shown in Figure 3a. The selected FE for the post-tensioned tendon is a uniaxial tension-only 3D spar element (Link10) with linear-elastic behavior. The device is simulated as connected to the supports of the model (foundation) and at the upper level of belfry to a perimetral load-distribution beam (Beam4) to have a uniform distribution of the pre-compression forces. This 3D uniaxial element has linear-elastic behavior with tension, compression, torsion, and bending capabilities. The prestressing force is applied at the tendons by means of strains. This technique is more realistic to account for restoring forces at

the tendon than only applying external normal forces. Restoring forces have a high impact in the realistic simulation of prestressed masonry. This trend was investigated in detail by comparing externally prestressed walls in laboratory and numerically by Sperbeck (2009). The nonlinear static analyses are carried out as aforementioned (Section 7) in combination of the masonry material model of Gambarotta and Lagomarsino (1997) by means of subroutines.

For similitude of results only the corresponding to the high prestressing level are presented ( $0.30F_v$ ). It is worth noting at the comparative of failure mechanisms of Figures 5, 6 and 8 that prestressing considerably reduces damage at belfry. The seismic performance is enhanced by increasing force, displacement and confinement as shown at the comparative of capacity curves of Figure 8 and Tables 5 and 6. It is observed an upgrading of 35% of displacement (30.2% of force) at the  $-X$  model and 20% of displacement (21.5% of force) at the constrained  $+X$  model. With these results it is corroborated that external vertical prestressing allows a substantial increment of the ductility of historical masonry towers and may be transformed into a high energy dissipation system by the formed loop at the capacity curve. The assessment and risk reduction summaries are presented in Tables 5 and 6. The seismic coefficient of the  $-X$  model in original state (0.126) is in good agreement with the obtained by Preciado, 2007 (0.120) by means of 3D limit analysis approach, as well as with the observed damages after passed EQs. At ULS no crushing is observed:  $-X$  original state 1.80 MPa, retrofitted 2.38 MPa;  $+X$  original state 1.15 MPa, retrofitted 1.48 MPa. In all cases (original state and prestressed condition) the obtained compressive stresses are lower than the intrinsic strength of 2.5 MPa. In the seismic evaluations of the bell-towers by the CS method of Figure 9, it is worth noting that the retrofitted tower is able to withstand a seismic action in  $-X$  thanks to the energy dissipation enhancement, but not enough in  $+X$  due to the façade constraint. Even by applying a medium prestressing level

( $0.15F_v$ ) that allows more ductility enhancement, the maximum obtained displacement of 100 mm is lower than the target one of 105 mm (Table 7). To bring the additional ductility, a combination of the Technora prestressing devices with an internal wrapping of belfry (GFRP sheets) is suggested.

## 9. CONCLUSIONS

Masonry is a heavy and highly heterogeneous material and presents brittle failure and nonlinear behavior since very low lateral loads due to its poor tensile strength compared to compression. This generates a lack of good connection between structural elements and the great structural mass induces high inertia forces in EQ conditions. The failure modes mainly depend of the EQ source and frequencies, geometry, materials, structural type and lack of rigid diaphragms. Seismic upgrading of URM old buildings has to be designed by engineering techniques and compatible materials fully removable for respecting the architectonic value of the building. The main objective is to increase its ultimate lateral load capacity and ductility for energy dissipation purposes. The methodology was applied on two Colonial masonry towers in Colima, Mexico, characterized for its high seismicity ( $EQ > M7.5$ ). The possibility to accurately calibrate the numerical FE model with real experimental data highlighted the use of this approach in comparison to analytical methods. Seismic analyses by calibrated FE models were developed considering two directions (-X and +X). The nonlinear analyses were developed by the pushover method to obtain the failure modes and to compare the seismic upgrading between the original condition and retrofitted. The capability of the applied material model to simulate the nonlinear behavior of masonry was validated and showed a satisfactory agreement. The huge impact of the low tensile strength of masonry and large openings at belfries on the seismic behavior was observed. Compared to the brittle constrained +X model, the -X model presented its

characteristic bending behavior due to the disconnection with the façade, represented by 25% of more displacement capability. The +X model was more resistant to horizontal loading, but less ductile, which is not relevant for seismic energy dissipation purposes. It was also applied the CS method to compare the equivalent SDOF system with the seismic demand. The maximum reached displacement for both models was not enough to withstand the seismic demand. The maximum performance of the -X model was of about 19% less than the required performance and even more drastic in the +X model (40% less). The URM was converted into a high-dissipative reinforced masonry by the addition of external vertical prestressing at key points of the structure identified in the seismic vulnerability assessment. This technique is in compliance with the demand for architectural conservation and may be located horizontally and vertically without bonding in order to be fully removable. Taking into account the parametric study of Preciado (2011), the Colonial towers were retrofitted with four prestressing devices of FRPs. The total prestressing force was calculated taking into account percentages of the vertical loading of the tower. The prestressing force was applied at the tendons by means of strains. This technique is more realistic to account for restoring forces at the tendon than only applying external normal forces. The seismic performance was enhanced by increasing force, displacement and internal confinement as shown at the comparative of capacity curves. It was observed an upgrading of 35% of displacement at the -X model and 20% of displacement at the constrained +X model. With these results it was corroborated that external vertical prestressing allows a substantial increment of the ductility of historical masonry towers and may be transformed into a high energy dissipation system. The seismic coefficient of the -X model in original state was in good agreement with the obtained by other researchers. At ULS no crushing was observed in the -X and +X model in original state and retrofitted. In the seismic evaluations by the CS method, the retrofitted tower was able to withstand a seismic action in -X thanks to the energy dissipation

enhancement, but not enough in +X due to the façade constraint. To bring the additional ductility, a combination of vertical prestressing with an internal wrapping of belfry was suggested.

## REFERENCES

- Ascione, L., Feo, L. and Fraternali, F (2005). “Load carrying capacity of 2D FRP/strengthened masonry structures.” *Composites Part B: Engineering*, 36(8): 619–26.
- Bandy, W., Mortera-Gutierrez, C., Urrutia-Fucugauchi, J. and Hilde, T. W. C. (1995). “The subducted Rivera-Cocos plate boundary: Where is it, what is it, and what is its relationship to the Colima rift?” *Geophysical Research Letters*, 22: 3075-3078.
- Barbat, A. H., Pujades, L. G. and Lantada, N. (2008). “Seismic Damage Evaluation in Urban Areas Using the Capacity Spectrum Method: Application to Barcelona”. *Journal of Soil Dynamics and Earthquake Engineering*, 28: 851-865.
- Barbieri, G., Biolzi, L., Bocciarelli, M., Fregonese, L. and Frigeri, A. (2013) “Assessing the seismic vulnerability of a historical building.” *Engineering Structures*, 57: 523–535.
- Bayraktar, A., Türker, T., Sevim, B., Altunisik, A. C. and Yildirim, F. (2009). “Modal parameter identification of Hagia Sophia bell-tower via ambient vibration test.” *Journal of Nondestructive Evaluation* 28: 37-47.
- Biolzi, L., Ghittoni, C., Fedele, R. and Rosati, G. (2013). “Experimental and theoretical issues in FRP-concrete bonding.” *Construction Building Materials*, 41: 182–190.
- Blasi, C. and Foraboschi, P. (1994). “Analytical approach to collapse mechanisms of circular masonry arch.” *Journal of Structural Engineering (ASCE)*, 120(8): 2288-2309.
- Calderini, C. and Lagomarsino, S. (2006). “A micromechanical inelastic model for historical masonry.” *Journal of Earthquake Engineering* 10(4): 453-479.
- Carreño, M. L., Cardona, O. D. and Barbat, A. H. (2007). “Urban Seismic Risk Evaluation: A Holistic Approach”. *Journal of Natural Hazards*, 40: 137-172.
- Carreño, M. L., Cardona, O. D. and Barbat, A. H. (2012). “New methodology for urban seismic risk assessment from a holistic perspective”. *Bulletin of Earthquake Engineering*, 10: 547-565.



Castellano, M. G. (2001). "Innovative technologies for earthquake protection of architectural heritage." Proceedings of the International Millennium Congress: More than two thousand years in the history of Architecture, UNESCO-ICOMOS, Paris, France.

Crisafulli, F. J. and Carr, A. J. (2007). "Proposed macro-model for the analysis of infilled frame structures." Bulletin of the New Zealand Society for Earthquake Engineering, 40(2): 69-77.

D'Ambrisi, A., Focacci, F. and Caporale, A. (2013a). "Strengthening of masonry-unreinforced concrete railway bridges with PBO-FRCM materials." Composite Structures, 102: 193-204.

D'Ambrisi, A., Feo, L. and Focacci, F. (2013b). "Experimental and analytical investigation on bond between Carbon-FRCM materials and masonry." Composite Structures, 46: 15-20.

Eurocode 8 (2004). "Design of structures for earthquake resistance - Part 1: General rules, seismic actions and rules for buildings." European Standard.

Fajfar, P. (2000). "A nonlinear analysis method for performance-based seismic design." Journal of Earthquake Spectra, 16(3): 573-591.

Fedele, R., Scaioni, M., Barazzetti, L., Rosati, G. and Biolzi, L. (2014). "Delamination tests on CFRP-reinforced masonry pillars: Optical monitoring and mechanical modeling." Cement and Concrete Composites, 45: 243-254.

Foraboschi P. (2013). "Church of San Giuliano di Puglia: Seismic repair and upgrading." Engineering Failure Analysis 33: 281-314.

Foraboschi, P. and Vanin, A. (2013a). "Non-linear static analysis of masonry buildings based on a strut-and-tie modeling." Soil Dynamics and Earthquake Engineering, 55: 44-58.

Foraboschi, P. and Vanin, A. (2013b). "New methods for bonding FRP strips onto masonry structures: experimental results and analytical evaluations." Composites: Mechanics, Computations, Applications, An International Journal, 4(1): 1-23.

Ganz, H. R. (1990). "Post-tensioned masonry structures: Properties of masonry design considerations post-tensioning system for masonry structures applications." VSL Report Series No. 2, Berne, Switzerland.

Ganz, H. R. (2002). "Post-tensioned masonry around the world." Proceedings of the first annual Conference of the Post-tensioning Institute, San Antonio, USA.

Gambarotta, L. and Lagomarsino, S. (1997). "Damage models for the seismic response of brick masonry shear walls." Part I and II. *Earthquake Engineering and Structural Mech.* 26: 441-462.

Grünthal, G. (1998). "European Macroseismic Scale EMS-98." Notes of the European Center of Geodynamics and Seismology, Vol. 15, Luxembourg.

INAH (2003). "Restoration and strengthening works on the damaged historical buildings after the 2003 Colima, Mexico earthquake." National Institute of Anthropology and History, Mexico.

Indirli, M., Castellano, M. G., Clemente, P. and Martelli, A. (2001). "Demo-application of Shape Memory Alloy Devices: The rehabilitation of the S. Giorgio church bell-tower." *Proceedings of SPIE, Smart Structures and Materials.*

Ivorra, S. and Pallares F. J. (2006). "Dynamic investigations on a masonry bell tower." *Engineering structures*, 28: 660-667.

Ivorra, S., Pallares, F. J. and Adam, J. M. (2008). "Experimental and numerical studies on the bell tower of Santa Justa y Rufina (Orihuela-Spain)." *Proceedings of the 6th International Conference on Structural Analysis of Historical Constructions (SAHC)*, Bath, UK.

Lantada, N., Pujades, L. and Barbat, A. (2009). "Vulnerability index and Capacity Spectrum based methods for urban seismic risk evaluation. A comparison". *Journal of Natural Hazards*, 51: 501-524.

Lofti, H. R. and Shing, P. B. (1994). "Interface model applied to fracture of masonry structures." *Journal of Structural Engineering*, 120(1): 63-81.

Lourenço, P. B. and Rots, J. (1997). "A multi-surface interface model for the analysis of masonry structures." *Journal on Engineering Mechanics*, 123(7): 660-668.

Lourenço, P. B., Rots, J. and Blaauwendraad, J. (1998). "Continuum model for masonry: Parameter estimation and validation." *Journal on Structural Engineering*, 124(6): 642-652.

MDS-CFE (2008). "Manual of Civil Constructions: Seismic Design (in Spanish)." Federal Commission of Electricity (CFE) and Institute of Electrical Research, Mexico.

Mondal, G. and Jain, S. K. (2008). "Lateral stiffness of masonry infilled reinforced concrete frames with central openings." *Earthquake Spectra*, 24(3): 701-723.

Muciaccia, G. and Biolzi, L. (2012). "Thermal degradation of fiber reinforced extruded materials." *Fire Safety Journal*, 49(4): 89-99.

NCSE (2002). "Spanish Seismoresistant Construction Norm (in Spanish)." General Part and Edification (Spanish standard). Ministry of Foment. Spain.

NTCDF (2004). "Complementary Technical Norms of the Mexican Construction Code (in Spanish)." Mexico.

Orduña, A. and Lourenço, P. B. (2005a). "Three-dimensional limit analysis of rigid blocks assemblages. Part I: Torsion failure on frictional interfaces and limit analysis formulation." *International Journal of Solids and Structures*, 42(18-19): 5140-5160.

Orduña, A. and Lourenço, P. B. (2005b). "Three-dimensional limit analysis of rigid blocks assemblages. Part II: Load-path following solution procedure and validation." *International Journal of Solids and Structures*, 42(18-19): 5161-5180.

Orduña, A., Preciado, A., Galván, J. F. and Araiza, J. C. (2008). "Vulnerability assessment of churches at Colima by 3D limit analysis models." *Proceedings of the 6th Int. Conference on Structural Analysis of Historical Constructions (SAHC)*, Bath, UK.

Pandey, B. H. and Meguro, K. (2004). "Simulation of brick masonry wall behavior under in-plane lateral loading using applied element method." *Proceedings of the 13th Conference on Earthquake Engineering*, Paper 1664, Vancouver, Canada.

Preciado, A. (2007). "Seismic vulnerability assessment of historical constructions in the State of Colima, Mexico (in Spanish)." Master thesis, University of Colima, Mexico.

Preciado (2011). "Seismic vulnerability reduction of historical masonry towers by external prestressing devices". Doctoral thesis, Technical University of Braunschweig, Germany and University of Florence, Italy.

Preciado, A., Lester, J., Ingham, J. M., Pender, M. and Wang, G. (2014). "Performance of the Christchurch, New Zealand Cathedral during the M7.1 2010 Canterbury earthquake." *Proceedings of the 9th International Conference on Structural Analysis of Historical Constructions (SAHC)*, Topic 11, Paper 02, Mexico City.

Preciado and Orduña (2014). “A correlation between damage and intensity on old masonry churches in Colima, Mexico by the 2003 M7.5 earthquake.” *Journal of Case Studies in Structural Engineering*, 2: 1-8.

Pujades, L. G. (2012). “Seismic performance of a block of buildings representative of the typical construction in the Example district in Barcelona, Spain”. *Bulletin of Earthquake Engineering*, 10(1): 331-349.

Ramirez-Gaytan A. (2008). “Modeling of the source and simulation of accelerograms of the earthquake of Tecoman of the 21st of January, 2003, by the method of the empirical Green’s function (in Spanish).” Doctoral thesis, National Autonomous University of Mexico (UNAM).

Rodriguez-Lozoya, H., Quintanar, L., Rebollar, C., Gomez, J, Yagi, Y., Dominguez, T., Reyes, G., Javier, C. and Alcantara, L. (2007). “Source characteristics of the 22nd January 2003 Mw 7.5 Tecoman, Mexico, earthquake and its rupture process”. *Journal of Geophysical Research*.

Schlegel, R. (2004). “Numerical simulations of masonry structures by homogenized and discrete modeling strategies (in German).” Doctoral thesis, University of Weimar, Germany.

Sperbeck, S. (2009). “Seismic risk assessment of masonry walls and risk reduction by means of prestressing.” Doctoral thesis, Technical University of Braunschweig, Germany.

SSN (2010). National Seismological Service of the National Autonomous University of Mexico (UNAM).

UCOL (1997). “The macro-earthquake of Manzanillo occurred on October 9th, 1995 (in Spanish).” University of Colima (UCOL), Government of the state of Colima and the Mexican Society of Seismic Engineering.

## LIST OF FIGURES

Figure 1: The Cathedral of Colima; (a) observed damage after the 1941 M7.6 earthquake and (b) crack pattern by the 2003 M7.5 earthquake

Figure 2: Seismic hazard of Colima; (a) seismic hazard of Mexico, low (A)-very high (D) (MDS-CFE, 2008) and (b) Tectonic map of Occidental Mexico (Bandy et al., 1995)

Figure 3: Dynamic experimental campaigns at left belfry; (a) general view of the Cathedral and position of vibration tests and arrangement of prestressing and (b) arrangement of sensors

Figure 4: Mortar joint and brick failure domains (Gambarotta and Lagomarsino, 1997)

Figure 5: Comparison of principal plastic strains (front and back) at a displacement of 100 mm for a seismic action in  $-X$  (S-N): (a) original (ULS) and (b) retrofitted  $0.30F_v$

Figure 6: Comparison of principal plastic strains (front and back) at a displacement of 75 mm for a seismic action in  $+X$  (N-S): (a) original (ULS) and (b) retrofitted  $0.30F_v$

Figure 7: Comparison of capacity curves in original state for a seismic action in  $-X$  and  $+X$  with the damage grades (EMS-98) and limit states (EC-8)

Figure 8: Comparison of capacity curves in original state and retrofitted ( $0.30F_v$ ) with the damage grades (EMS-98) and limit states (EC-8): (a)  $-X$  and (b)  $+X$  springs

Figure 9: Seismic evaluation of the north bell tower of the Cathedral of Colima by the Capacity Spectrum method: (a)  $-X$  direction and (b)  $+X$  direction (springs)

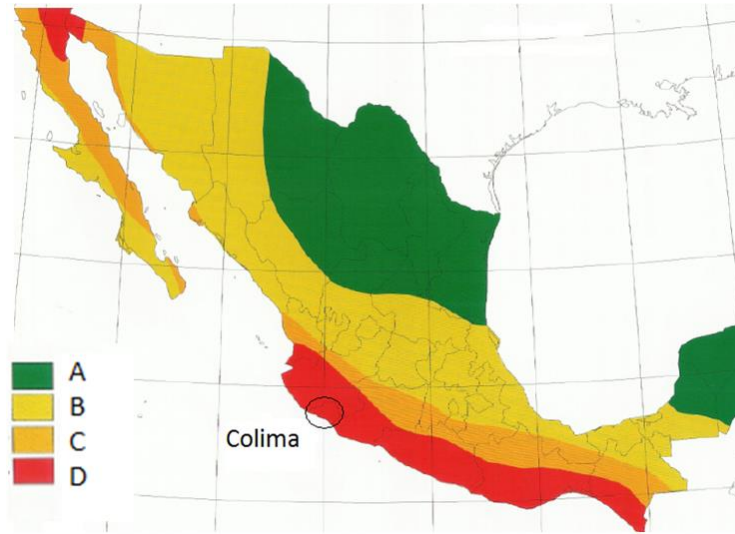


(a)

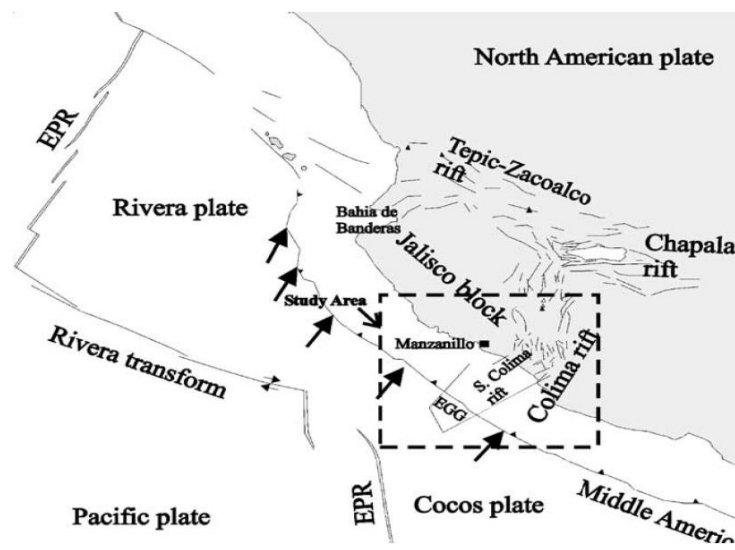


(b)

Figure 1: The Cathedral of Colima; (a) observed damage after the 1941 M7.6 earthquake and (b) crack pattern by the 2003 M7.5 earthquake



(a)

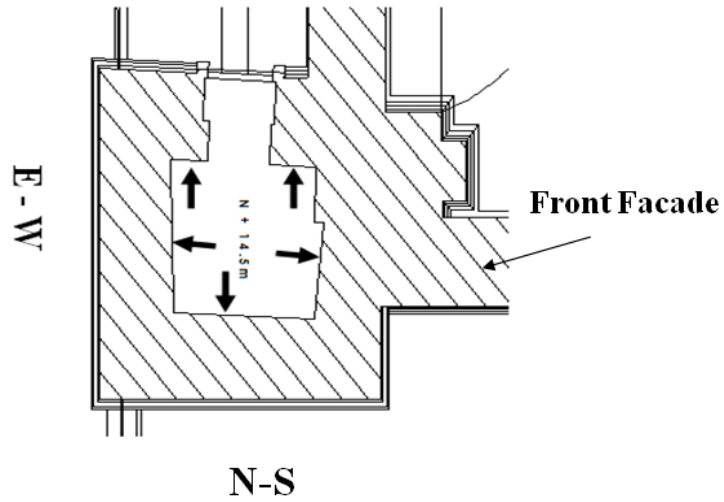


(b)

Figure 2: Seismic hazard of Colima; (a) seismic hazard of Mexico, low (A)-very high (D) (MDS-CFE, 2008) and (b) Tectonic map of Occidental Mexico (Bandy et al., 1995)



(a)



(b)

Figure 3: Dynamic experimental campaigns at left belfry; (a) general view of the Cathedral and position of vibration tests and arrangement of prestressing and (b) arrangement of sensors



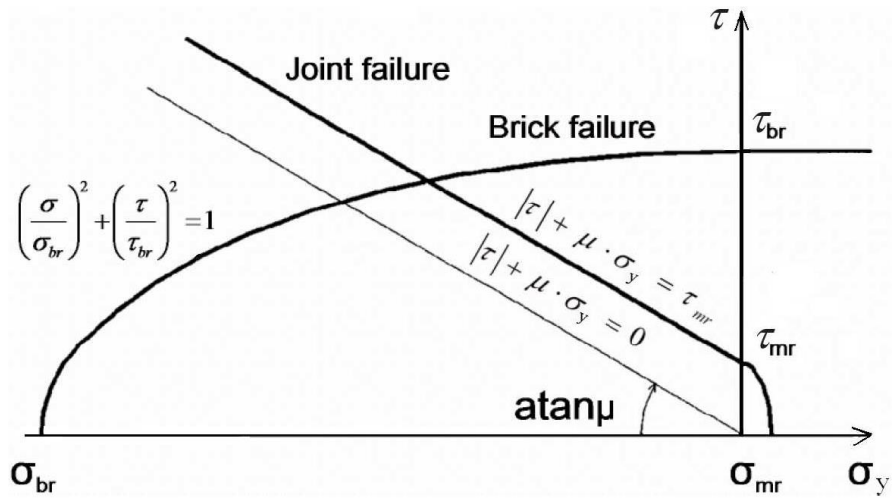


Figure 4: Mortar joint and brick failure domains (Gambarotta and Lagomarsino, 1997)

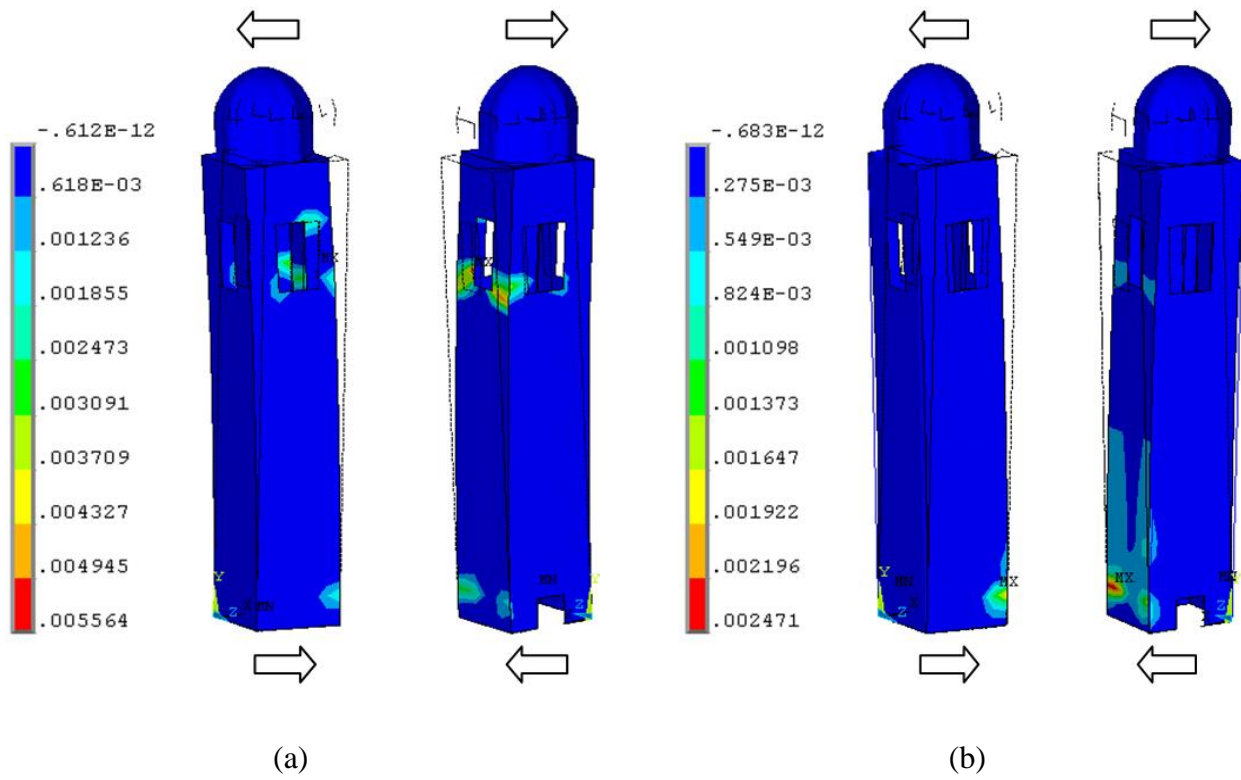


Figure 5: Comparison of principal plastic strains (front and back) at a displacement of 100 mm for a seismic action in  $-X$  (S-N): (a) original (ULS) and (b) retrofitted  $0.30F_v$

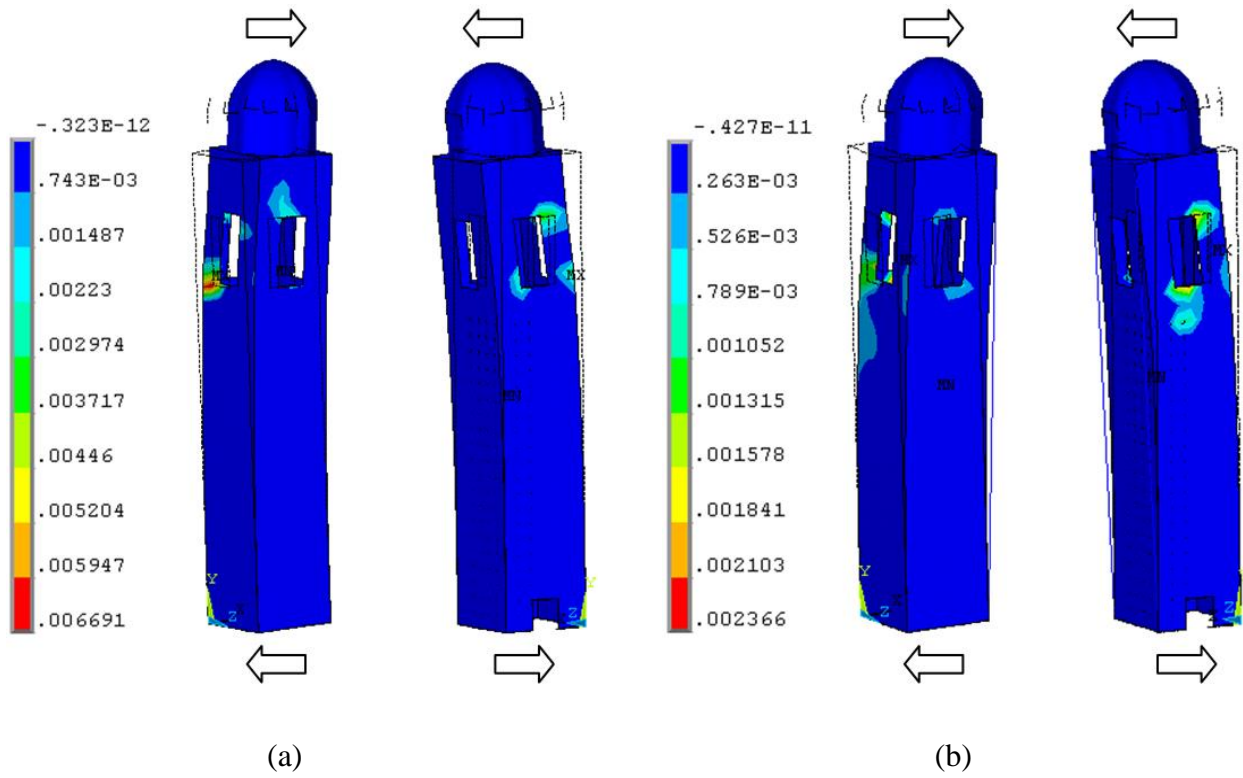


Figure 6: Comparison of principal plastic strains (front and back) at a displacement of 75 mm for a seismic action in +X (N-S): (a) original (ULS) and (b) retrofitted 0.30Fv

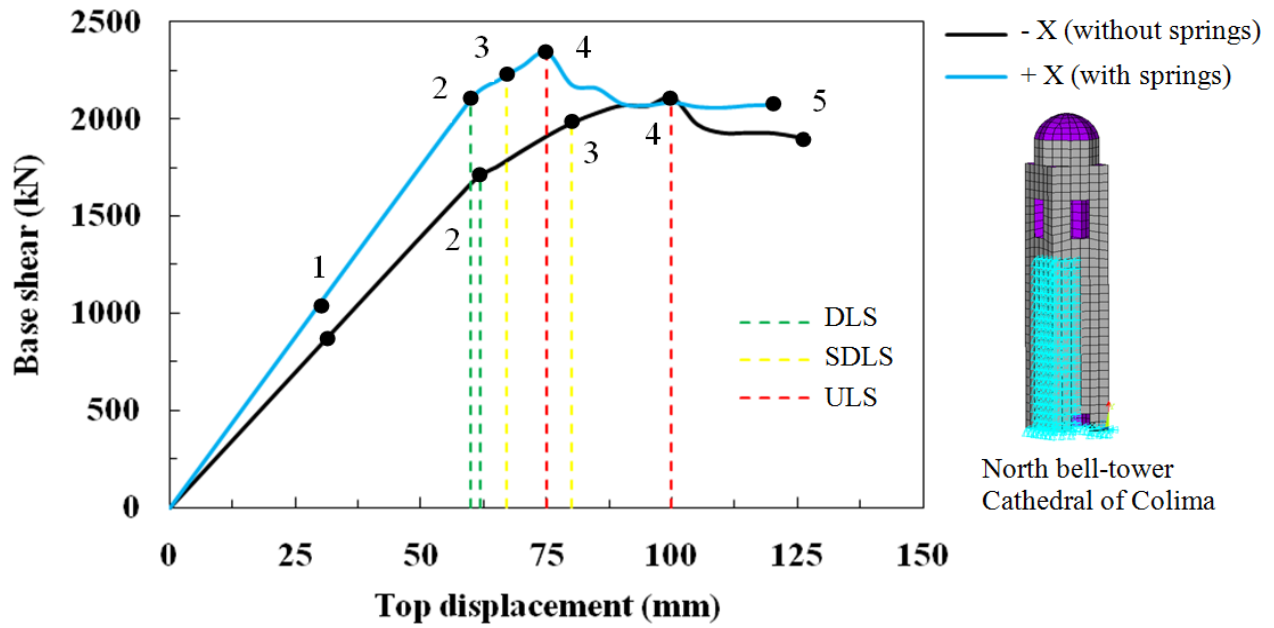
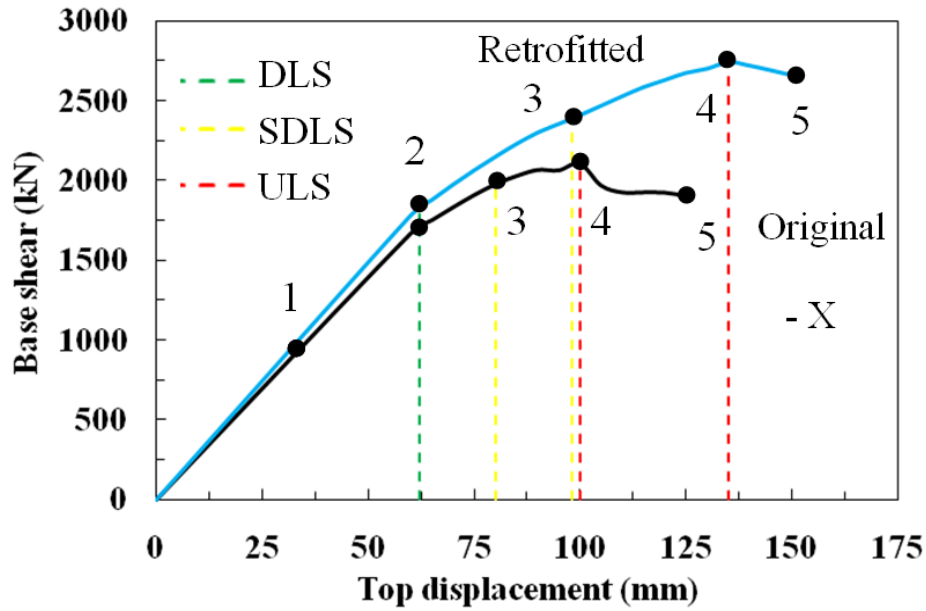
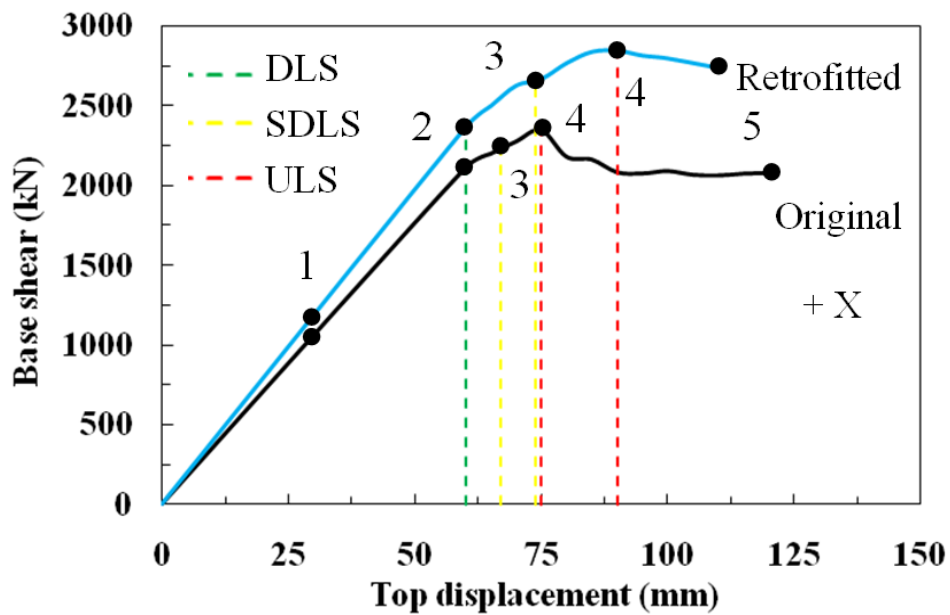


Figure 7: Comparison of capacity curves in original state for a seismic action in  $-X$  and  $+X$  with the damage grades (EMS-98) and limit states (EC-8)

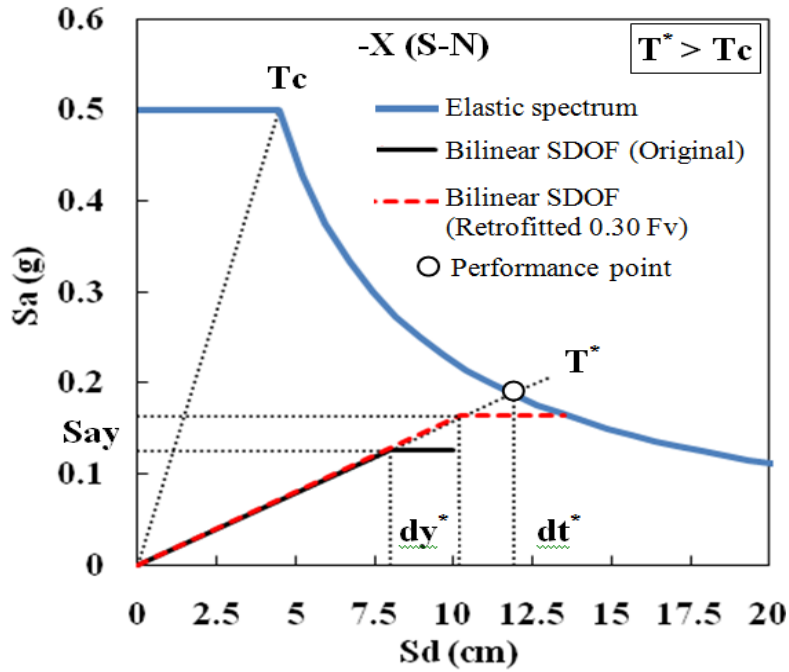


(a)

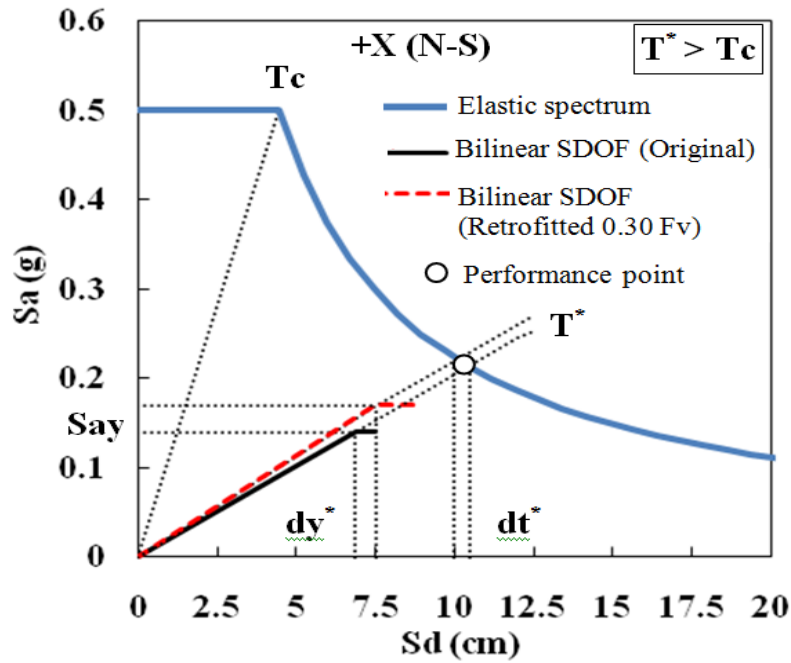


(b)

Figure 8: Comparison of capacity curves in original state and retrofitted (0.30Fv) with the damage grades (EMS-98) and limit states (EC-8): (a) -X and (b) +X springs



(a)



(b)

Figure 9: Seismic evaluation of the north bell tower of the Cathedral of Colima by the Capacity

Spectrum method: (a) -X direction and (b) +X direction (springs)

## **LIST OF TABLES**

Table 1: Information of the principal strong earthquakes occurred in Colima, Mexico (UCOL et al., 1997), and (Rodriguez-Lozoya et al., 2007)

Table 2: Parameters describing the elastic response spectrum for the Colima City center

Table 3: Numerical vs. experimental frequencies

Table 4: Summary of masonry inelastic parameters for the material model

Table 5: Seismic assessment summary of the north bell tower in original state and retrofitted  $0.30F_v$  for an earthquake action in  $-X$  and  $+X$  (springs)

Table 6: Seismic risk reduction comparison between original state and retrofitted ( $0.30F_v$ ) by the increment of  $F$ ,  $U$  and  $S.C.$  for an earthquake in  $-X$  and  $+X$  (springs)

Table 7: Seismic evaluation summary of the bell tower using the Capacity Spectrum method, original state against retrofitting with FRP external prestressing

Table 1: Information of the principal strong earthquakes occurred in Colima, Mexico (UCOL et al., 1997), and (Rodriguez-Lozoya et al., 2007)

<b>No</b>	<b>Date</b>	<b>Latitude N</b>	<b>Longitude W</b>	<b>Magnitude Mw</b>	<b>Intensity MMI Colima City</b>	<b>Comment</b>
1	03.06.1932	19.80°	104.00°	8.0	VIII	R and NA
2	18.06.1932	18.95°	104.42°	7.8	IX	Replica of 1
3	15.04.1941	18.85°	102.94°	7.6	X	C and NA
4	30.01.1973	18.39°	103.21°	7.6	VIII	C and NA
5	09.10.1995	18.79°	104.47°	8.0	VII	R and NA
6	21.01.2003	18.63°	104.13°	7.5	VIII	C and NA

Plates that generated the earthquake: R= Rivera; NA= North American; C= Cocos



Table 2: Parameters describing the elastic response spectrum for the Colima City center

<b>Seismic hazard</b>	<b>Ground type</b>	$a_0(g)$	$c$	$T_a$ (s)	$T_b$ (s)	$r$
zone D	I	0.5	0.5	0.0	0.6	1

Table 3: Numerical vs. experimental frequencies

<b>Mode type</b>	<b>Experimental Frequency (Hz)</b>	<b>FE Frequency (Hz)</b>	<b>Error (%)</b>
1 <sup>st</sup> flexural E-W	1.4067	1.4193	0.89
1 <sup>st</sup> flexural N-S	1.6222	1.6174	0.30

Table 4: Summary of masonry inelastic parameters for the material model

<b>Parameter</b>	<b>Value</b>	<b>Unit</b>
$\sigma_m$ : tensile strength for mortar	0.25	MPa
$\tau_m$ : shear strength for mortar	0.35	MPa
$c_m$ : shear inelastic compliance for mortar	1	-
$\beta_m$ : softening coefficient for mortar	0.7	-
$\mu$ : friction coefficient for mortar	0.6	-
$\sigma_M$ : compressive strength of masonry	2.5	MPa
$\tau_b$ : shear strength of units	1.5	MPa
$c_M$ : inelastic compliance of masonry in compression	1	-
$\beta_M$ : softening coefficient of masonry	0.4	-

Table 5: Seismic assessment summary of the north bell tower in original state and retrofitted

0.30F<sub>v</sub> for an earthquake action in -X and +X (springs)

Ref.	Limit states EC-8 and Damage grades EMS-98												S.C. OS	S.C. R
	DLS (DG 2)				SDLS (DG 3)				ULS (DG 4)					
	<i>F<sub>OS</sub></i>	<i>U<sub>OS</sub></i>	<i>F<sub>R</sub></i>	<i>U<sub>R</sub></i>	<i>F<sub>OS</sub></i>	<i>U<sub>OS</sub></i>	<i>F<sub>R</sub></i>	<i>U<sub>R</sub></i>	<i>F<sub>OS</sub></i>	<i>U<sub>OS</sub></i>	<i>F<sub>R</sub></i>	<i>U<sub>R</sub></i>		
- X	1740	62	1820	62	1970	80	2380	98	2105	100	2741	135	0.126	0.164
+ X	2108	60	2368	60	2240	67	2650	74	2345	75	2849	90	0.140	0.170

OS: original state; R: retrofitted; S.C: seismic coefficient; F (kN); U (mm)

Table 6: Seismic risk reduction comparison between original state and retrofitted (0.30F<sub>v</sub>) by the increment of F, U and S.C. for an earthquake in -X and +X (springs)

FE model reference	Limit states EC-8 and Damage grades EMS-98						Seismic Coefficient %
	DLS (DG 2)		SDLS (DG 3)		ULS (DG 4)		
	<i>F</i> %	<i>U</i> %	<i>F</i> %	<i>U</i> %	<i>F</i> %	<i>U</i> %	
-X	4.6	0.0	20.8	22.5	30.2	35.0	30.2
+X	12.3	0.0	18.3	10.5	21.5	20.0	21.4

Table 7: Seismic evaluation summary of the bell tower using the Capacity Spectrum method,  
original state against retrofitting with FRP external prestressing

<b>FE model reference</b>	<b>m* (Ton)</b>	<b>dy* (mm)</b>	<b>Fy* (Ton)</b>	<b>Say (g)</b>	<b>dm* (mm)</b>	<b>dt* (mm)</b>	<b>Comment</b>
<b>-X Original state</b>	1707.4	80	215	0.126	100	119.2	Loss of belfry
<b>-X Retrofitted 0.30 Fv</b>	1707.4	102	279.4	0.164	135	119.2	Reparable
<b>+X Original state</b>	1707.4	68.5	239	0.140	75	105	Loss of belfry
<b>+X Retrofitted 0.30 Fv</b>	1707.4	75	290.5	0.170	90	100	Loss of belfry

m\*: mass; dy\*: yield displacement; Fy\*: yield force; Say: yield acceleration; dm\*: maximum displacement; dt\*: target displacement (performance point)